Fault heterogeneity and earthquake scaling

Alison Hetherington[1] and Sandy Steacy[1]

[1] There is an on-going debate in the seismological community as to whether stress drop is independent of earthquake size and this has important implications for earthquake physics. Here we investigate this question in a simple 2D cellular automaton that includes heterogeneity. We find that when the range of heterogeneity is low, the scaling approaches that of constant stress drop. However, clear deviations from the constant stress drop model are observed when the range of heterogeneity is large. Further, fractal distributions of strength show more significant departures from constant scaling than do random ones. Additionally, sub-sampling the data over limited magnitude ranges can give the appearance of constant stress drop even when the entire data set does not support this. Our results suggest that deviations from constant earthquake scaling are real and reflect the heterogeneity of natural fault zones, but may not provide much information about the physics of earthquakes. **Citation:** Hetherington, A., and S. Steacy (2007), Fault heterogeneity and earthquake scaling, *Geophys. Res. Lett.*, *34*, L16310, doi:10.1029/2007GL030365.

1. Introduction

[2] Whether rupture processes differ between large and small earthquakes is of fundamental importance in earthquake physics and has important implications for earthquake predictability. Observations of power-law magnitude frequency distributions, similarities in the nucleation processes of large and small earthquakes [*Abercrombie and Mori*, 1994], and the concept of self-organized criticality have all been used to support the argument that no significant difference exists. Other observations, however, such as a bump (excess number of large earthquakes) in the magnitude-frequency distribution [e.g., *Stirling et al.*, 1996] and the possibility that earthquakes begin with slow slip, the duration of which scales with the eventual earthquake size [*Ellsworth and Beroza*, 1995], have been used to support exactly the opposite view.

[3] Over the past several years, this debate has extended into the question of "earthquake scaling", in particular whether average stress drops are the same for large and small earthquakes; if they were this would support the argument of self-similar rupture processes. Studies have been undertaken using a variety of methods, involving both new data [e.g., *Abercrombie*, 1995] and applying new methods to existing data [e.g., *Beeler et al.*, 2003]. The data are usually collected over a limited range of magnitudes and have been analysed both in terms of energy scaling in plots of seismic energy vs. moment [e.g., *Ide and Beroza*, 2001] and in terms of stress scaling with graphs of seismic moment vs. source radius [e.g., *Abercrombie*, 1995]. To date the results have been inconclusive.

[4] *Mayeda and Walter* [1996] analysed 48 earthquakes in the range M = 3.3 − 7.3 from the western US and found that stress drop increased approximately with $M_o^{0.25}$. In an analysis of 41 M = 0.5 − 5. earthquakes in the Long Valley Caldera, *Prejean and Ellsworth* [2001] found that radiated energy similarly increased with seismic moment and suggested that this meant that large earthquakes were more efficient than small ones. An earlier study, by *Abercrombie* [1995] of over 100 events between M = −1. − 5.5 was more ambiguous in that both constant stress drop and an increase in energy with moment were observed; however she concluded that the latter may have due to errors in computing the seismic energy.

[5] By contrast, *Ide and Beroza* [2001] examined 6 previously published data sets, re-analysing 3 of them by adjusting for potentially missing energy. They found a nearly constant ratio of radiated energy to seismic moment over 17 orders of earthquake moment. *Abercrombie and Rice* [2005] carefully examined 30 well recorded earthquakes from Cajon Pass and found that while the data did suggest increased stress drop and seismic energy with increased moment, the errors in the data and the assumptions in the models precluded a clear resolution of the constant scaling controversy.

[6] Despite this uncertainty, a few authors have attempted to understand what might cause size dependency in earthquakes. *Beeler et al.* [2003] investigated the expected relationship between apparent stress and static stress drop and suggested that non-constant scaling may occur due to systematic variations in static stress drop, although they did not suggest what might cause such a pattern. Taking a different approach, a study by *Liu-Zeng et al.* [2005] modelled slip-length scaling, using a simple 1-D model of slip heterogeneity where stress drop was determined by the roll of a dice, and the length and width of the rupture were statistically linked to the slip. Their results suggested the possibility of a relationship between the level of heterogeneity and the slip-length scaling observed.

[7] Here we use a self-similar model to investigate the effects of heterogeneity on earthquake scaling. The model is a cellular automaton in which we impose the heterogeneity by controlling the patterns of cell strength using different fractal distributions and varying ranges of strength.

2. Methodology

[8] We investigate event scaling in a model with dimensions 512 by 64 cells and a cell-size of 0.25 km by 0.25 km to simulate a fault of 128 km length by 16 km width. We set the minimum strength of the cells at 1 MPa and

systematically vary the maximum strength and distribution of heterogeneity.

[9] Rather than iteratively adding the constant loading stress at each time step, an equivalent method has been developed which saves significant model run-time. The time to the first cell failure is determined by first calculating the time to failure $T(i)$ of each individual cell where i denotes the number of the cell:

$$T(i) = \frac{\sigma_f(i) - \sigma_{total}(i)}{\sigma_{load}} \qquad (1)$$

$\sigma_f(i)$ is the failure stress (strength) of that cell, $\sigma_{total}(i)$ is its current stress and σ_{load} is the stressing rate, here constant for all cells. We then determine the minimum $T(i)$ and denote this T_{jump} and use this to calculate the stress increase, σ_{jump}, to be added to all cells:

$$\sigma_{jump} = T_{jump} \times \sigma_{load} \qquad (2)$$

[10] The stress on each cells is then updated to $\sigma_{new}(i)$:

$$\sigma_{new}(i) = \sigma_{total}(i) + \sigma_{jump} \qquad (3)$$

leading to immediate rupture of the cell closest to failure.

[11] When a cell fails, its stress is redistributed according to the rules developed by *Steacy and McCloskey* [1999] that distribute more stress to unbroken neighbors than to those that have previously failed in the event. These rules were designed to produce a realistic stress concentration at the edges of the rupture which initially scales with the square root of the source radius and then asymptotically approaches a constant value, consistent with causing model earthquakes to propagate as slip pulses [*Heaton*, 1990]. An alternative stress concentration rule in which stress is only redistributed to unbroken cells [*Steacy and McCloskey*, 1998] produces similar results to those shown below for large ranges of heterogeneity. However, the stress concentrations are unrealistically high and hence this model is not explored in detail here.

[12] The redistributed stress may in turn cause neighbouring cells to fail and hence all contiguous cells that fail as the result of a single increment of stress are considered to be part of the same event. Note that cells recover their strength immediately (i.e. are instantaneously healed) and thus subsequent cell breakages result in complete stress drop.

[13] In order to calculate the size of each event, we first compute the average stress drop $(\Delta\overline{\sigma})$ by:

$$\Delta\overline{\sigma} = \frac{\sum \Delta\sigma}{N} \qquad (4)$$

where $\sum \Delta\sigma$ is the total stress drop for the event and N is the number of cells that failed at least once during it. Slip and seismic moment are calculated from the empirical relations of *Kanamori and Anderson* [1975]:

$$\overline{U} = \frac{16}{7\pi\mu} \Delta\overline{\sigma}\frac{r}{2} \qquad (5)$$

where the rigidity μ, is assumed to be 30 GPa and r is the rupture length (and source radius) determined from the

square root of the rupture area. Seismic moment is then calculated using:

$$M_0 = \mu\, A\, \overline{U} \qquad (6)$$

where A is the rupture area.

[14] To investigate the effects of heterogeneity we consider a range of models with different fractal dimensions (D = 1.4, 1.7, 2.0, 2.3) as well as random distributions over a variety of strength ranges. The maximum strength range is varied between 2–100 MPa. Ten realisations of each strength distribution are investigated. Each run is carried out for 5 million time-steps ensuring the occurrence of more than 50,000 events.

[15] The fractals are created using the method of *Turcotte* [1992], which allows fractals of a given dimension to be generated from a Gaussian random distribution that is filtered in the frequency domain by a user-specified parameter (β) that determines the fractal dimension. This distribution in turn depends on the seed to a random number generator and hence different realisations with the same fractal dimension can be generated by using different seeds, or the same seed can be used to create fractals with different dimensions; an example of the latter is shown in Figure 1.

[16] For each simulation we plot graphs of log seismic moment vs. log source radius and compute the slope from a least squares fit to the data. However, the large number of small events was found to dominate the line fit because the model produces a power-law distribution of event sizes. We therefore choose 10 random events for each source radius and use these values for the fit. If there are less than 10 values available, all of the data for that source radius are used. To ensure that the random selection of the 10 data does not control the fit, each random pick is carried out 10 times, and the average gradient of all the lines is calculated. In all cases the standard deviation of the 10 gradients was found to be around 0.05, tests of the standard deviation of 100 gradients were found to be on the same order. Typical examples of the fits to the data are shown in Figure 2.

3. Results

[17] We summarise our results in Figure 3 where we plot the mean slope vs. the maximum strength (which approximates the overall strength range as the minimum strength is held constant) for each of the fractal models as well as for the random distributions. All curves show the same general pattern in that the slope increases with increased strength range, however there are differences between the various heterogeneity distributions.

[18] Let us first examine the trend of the random strength distribution. At low strength ranges this has a gradient close to the value of constant stress drop (3.0) but it increases with increasing strength range to a value of approximately 3.25 at the maximum of 100 MPa. Our interpretation is that at low strength ranges, the strongest cells are equally likely to fail in small and large events, however as the strength range increases failure of the strongest cells is progressively confined to the largest events. This occurs because the strength difference between weak and strong cells is such that stress redistribution from weak cell failure is unlikely to
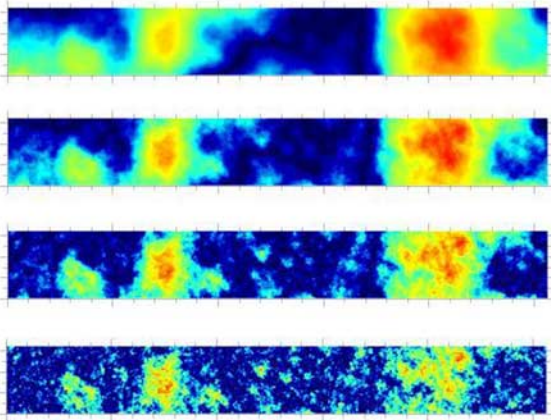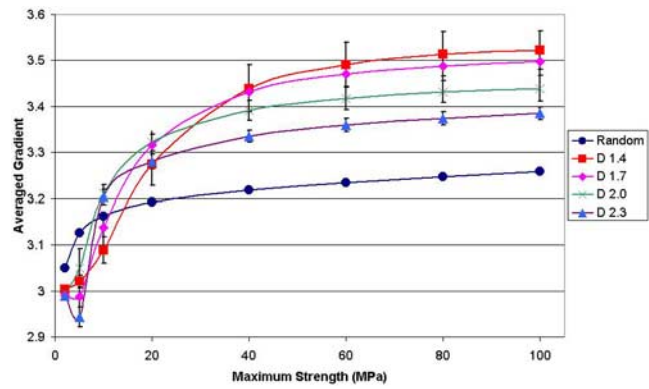
Figure 1. Strength distribution over the range 1–10 MPa for fractal dimensions (from top to bottom) D = 1.4, D = 1.7, D = 2.0, and D = 2.3.

Figure 3. Graph showing the average gradients of 10 realisations of each strength range and distribution. The error bars indicate the standard deviation for each set of realisations. The slope of constant stress drop is 3.0. The lines are shown for clarity and to highlight the crossovers between the gradients of the different models.

cause failure of the strongest cells in the absence of strong stress concentrations. Since the stress concentration increases with event size, strong cells become progressively more likely to break in larger events.

[19] For small strength ranges, the effect of strong cells failing in small events results in no difference in mean stress drop between large and small events and hence the slope is very close to 3. For large strength ranges, however, the mean stress drop increases as event size increases and this is reflected in a steeper gradient.

[20] Similar general trends are observed for the fractal distributions in that steeper slopes are observed for models with larger strength ranges and we believe this is explained by the above interpretation. However, a crossover is observed in that at low strength ranges the models with low fractal dimensions have lower gradients than those with high fractal dimensions whereas at large strength ranges the opposite is true.

[21] Our interpretation of the role of the strong patches (asperities) in the model on this cross-over in gradient is

based on visual inspection of ruptures at different strength ranges. At low ranges, the smallest slope occurs in models with a fractal dimension of 1.4. In these, we observe that events of all sizes can involve partial rupture of the asperities and hence there is little difference in the mean stress drop between large and small events. By contrast, in models with D = 2.3, large events generally involve complete failure of the asperities and thus, even though partial asperity failure is observed in the small events, there is a greater difference in mean stress drop between the large and small events and hence the gradient is steeper.

[22] At high strength ranges, we find, for fractal models D = 1.4, that very few small to medium sized ruptures involve breakage of the asperities, but that partial ruptures of these occur in the largest events. This leads to a strong increase in mean stress drop with event size and hence a steep slope. In the D = 2.3 models, however, we once again observe some participation of the asperities in the smaller events (although to a lesser extent than in the lower strength
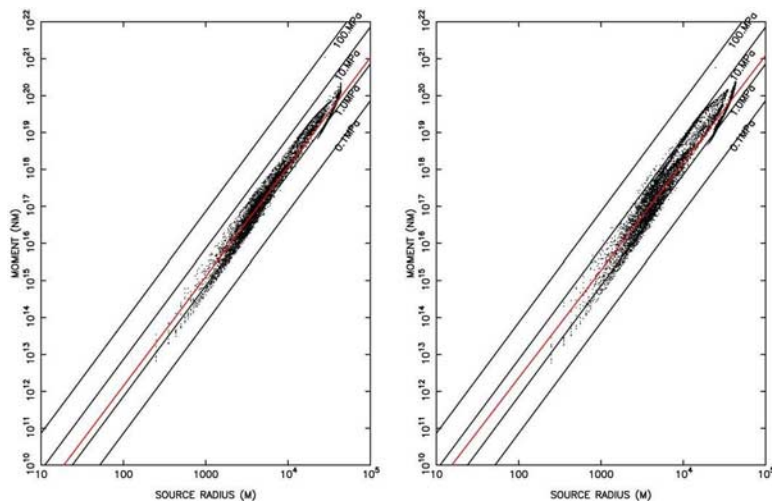
Figure 2. Moment vs. source radius for strength range 1–10 MPa. Fractal dimensions are (left) D = 1.4 and (right) D = 2.0. Lines of constant stress drop are shown in black ranging from 0.1 MPa to 100 MPa and the red line is the best fit to the data. Note the variation in moment release, and hence stress drop, over all but the very largest events.
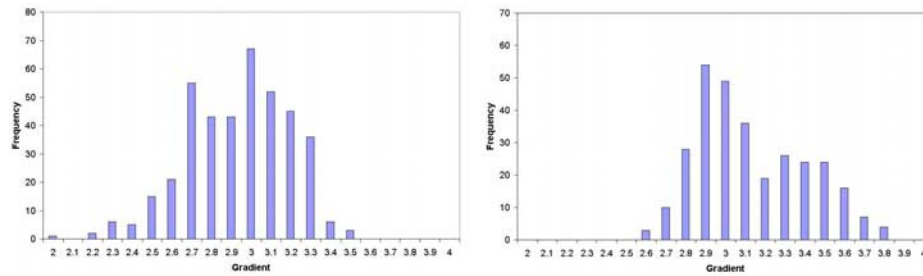
Figure 4. (left) Frequency of occurrence of gradients sampled over a restricted moment range, for a fractal distribution of 2.0 and a maximum strength of 10MPa. The data are divided into four seismic moment ranges; $<10^{15}$ Nm, $10^{15}-10^{17}$ Nm, $10^{17}-10^{19}$ Nm, and $>10^{19}$ Nm. Here the mean value is 2.93 and the median 2.97 while the gradient calculated over the entire data range is approximately 3.2. (right) Same as for Figure 4 (left), but sampled over 3 orders of seismic moment; $<10^{15}$ Nm, $10^{15}-10^{18}$ Nm, and $>10^{18}$ Nm. Note that the diagram contains fewer total fits due to the larger moment range. The histogram shows a shift to higher values with respect to Figure 4 (left) and has a mean value of 3.13 and median of 3.07.

ranges), while the largest tend to involve nearly complete asperity failure. This means that the difference in stress drop between large and small events is less than for the D = 1.4 models.

[23] In order to better compare our results with published analyses, we investigate the effects of small data sets by sub-sampling results from various models. Specifically, we randomly choose sets of 20 data points over a restricted range of event size (either 2 or 3 orders of seismic moment, consistent with *Ide and Beroza* [2001]) and calculate the slope for these 20 points. We repeat this 100 times for each moment range and in Figure 4 plot histograms of the frequency of occurrence of these gradients for one realisation of the model.

[24] The histograms show that for fractal distributions, using a restricted range of magnitudes results in much lower gradient values than those obtained using the full range of data. Additionally, increasing the magnitude range increases the gradients. This is not observed for the random strength distributions, however, because there is very little variation in magnitude for a given source radius and hence the errors due to sub-sampling are extremely small.

4. Discussion

[25] In a self-similar model in which the only difference between small and large events is that the latter develop greater stress concentrations, we find that – in the presence of heterogeneity – large events experience greater stress drops than small ones. Our interpretation is that strong patches (asperities) preferentially fail in large events due to the presence of larger stress concentrations.

[26] We further observe that sampling only small numbers of events over a limited magnitude range can erroneously lead to interpretations of constant or near-constant scaling, at least for the fractal models. This appears to be because these models exhibit considerable variations in moment release for any given source radius and hence a small sub-sample can lead to significant variability in the measured slope. The effect of sub-sampling decreases when the moment range over which the data are selected increases (even with the same number of data points).

[27] Our results suggest that increasing stress drop with increasing seismic moment may be a real phenomenon,

resulting from fault heterogeneity, but this departure from constant scaling does not require that there be differences in the physics of large and small earthquakes.

References

Abercrombie, R. E. (1995), Earthquake source scaling relationships from −1 to 5 ML using seismograms recorded at 2.5-km depth, *J. Geophys. Res.*, *100*(B12), 24,015−24,036.

Abercrombie, R. E., and J. Mori (1994), Local observations of the onset of a large earthquake: 28 June 1992 Landers, California, *Bull. Seismol. Soc. Am.*, *84*, 725−734.

Abercrombie, R. E., and J. R. Rice (2005), Can observations of earthquake scaling constrain slip weakening?, *Geophys. J. Int.*, *162*, 406−424.

Beeler, N. M., T. F. Wong, and S. H. Hickman (2003), On the expected relationships among apparent stress, static stress drop, effective shear fracture energy, and efficiency, *Bull. Seismol. Soc. Am.*, *93*, 1381−1389.

Ellsworth, W. L., and G. C. Beroza (1995), Seismic evidence for an earthquake nucleation phase, *Science*, *268*, 851−855.

Heaton, T. (1990), Evidence for and implications of self-healing pulses of slip in earthquake rupture, *Phys. Earth Planet. Inter.*, *64*(1), 1−20.

Ide, S., and G. C. Beroza (2001), Does apparent stress vary with earthquake size?, *Geophys. Res. Lett.*, *28*(17), 3349−3352.

Kanamori, H., and D. L. Anderson (1975), Theoretical basis of some empirical relations in seismology, *Bull. Seismol. Soc. Am.*, *65*, 1073−1095.

Liu-Zeng, J., T. Heaton, and C. DiCaprio (2005), The effect of slip variability on earthquake slip-length scaling, *Geophys. J. Int.*, *162*, 841−849.

Mayeda, K., and W. R. Walter (1996), Moment, energy, stress drop, and source spectra of western United States earthquakes from regional coda envelopes, *J. Geophys. Res.*, *101*(B5), 11,195−11,208.

Prejean, S. G., and W. L. Ellsworth (2001), Observations of earthquake source parameters at 2 km depth in the Long Valley Caldera, eastern California, *Bull. Seismol. Soc. Am.*, *91*, 165−177.

Steacy, S., and J. McCloskey (1998), What controls an earthquake's size?: Results from a heterogeneous cellular automaton, *Geophys. J. Int.*, *133*, F11−F14.

Steacy, S., and J. McCloskey (1999), Heterogeneity and the earthquake magnitude-frequency distribution, *Geophys. Res. Lett.*, *26*(7), 899−902.

Stirling, M. W., S. G. Wesnousky, and K. Kunihiko (1996), Fault trace complexity, cumulative slip, and the shape of the magnitude-frequency distribution for strike-slip faults−A global survey, *Geophys. J. Int.*, *124*, 833−868.

Turcotte, D. L. (1992), *Fractal and Chaos in Geology and Geophysics*, Cambridge Univ. Press, Cambridge, U. K.

A. Hetherington and S. Steacy, Geophysics Research Group, School of Environmental Sciences, University of Ulster, Coleraine BT52 1SA, Northern Ireland. (s.steacy@ulster.ac.uk)